Journal of Physics: Conference Series **500** (2014) 192014 doi:10.1088/1742-6596/500/19/192014

Modeling combined tension-shear failure of ductile materials

Y Partom
Retired from RAFARL, PO Box 2250, Haifa 31021, ISRAEL

E-mail: ypartom@netvision.net.il

Abstract. Failure of ductile materials is usually expressed in terms of effective plastic strain. Ductile materials can fail by two different failure modes, shear failure and tensile failure. Under dynamic loading shear failure has to do with shear localization and formation of adiabatic shear bands. In these bands plastic strain rate is very high, dissipative heating is extensive, and shear strength is lost. Shear localization starts at a certain value of effective plastic strain, when thermal softening overcomes strain hardening. Shear failure is therefore represented in terms of effective plastic strain. On the other hand, tensile failure comes about by void growth under tension. For voids in a tension field there is a threshold state of the remote field for which voids grow spontaneously (cavitation), and the material there fails. Cavitation depends on the remote field stress components and on the flow stress. In this way failure in tension is related to shear strength and to failure in shear. Here we first evaluate the cavitation threshold for different remote field situations, using 2D numerical simulations with a hydro code. We then use the results to compute examples of rate dependent tension-shear failure of a ductile material.

1. Introduction

Failure of ductile materials is usually expressed in terms of the effective plastic strain (ε^p_{eff}), or in terms of a time integral of a function of the effective plastic deformation rate (d^p_{eff}). There are many examples in the literature of such models and their calibration from tests [1-4]. On the other hand it is well known that ductile materials may fail by two different failure modes, shear failure and tensile failure. Shear failure has to do with shear localization and formation of shear bands. Shear localization starts at a certain value of ε^p_{eff}, when thermal softening overcomes strain hardening. It is therefore appropriate to express a shear failure criterion in terms of ε^p_{eff}. On the other hand, tensile failure comes about through void growth under tension. For a void in a quasi static tension field, there is a level of the remote field above which the void may grow spontaneously, and the material there fails. This level is the cavitation threshold, which depends on the remote field stress components, and on the local flow stress or shear strength. Failure in tension may therefore be related to shear strength and to failure in shear. In what follows we:

- Evaluate the cavitation threshold for different quasi static remote field situations, using 2D numerical simulations with a hydro code.
- Develop a combined tension-shear failure model based on the quasi static cavitation threshold, and using an overstress approach.
- Implement this failure model in a single cell computational tool, and run several examples to demonstrate how it works.

2. Cavitation threshold

Based on planar impact spall tests we assume that tensile failure may be caused by spontaneous growth of cavities (cavitation) in a tension field. We further assume that micron and sub micron cavities always exist in metals. The quasi static growth of a cavity by internal pressure in spherical and cylindrical symmetries has been worked out analytically long ago [5]. The similar problem with a remote tension field can be worked out in the same way, and the results are almost the same. The picture emerging from these solutions is: (1) Cavity growth is a shear strength dependent problem, and all its growth features depend on the flow stress, (2) Below a threshold tension P_c the cavity reaches equilibrium, and above P_c the cavity grows spontaneously without limit.

Beyond the cavitation threshold cavities grow, porosity increases, and at a certain porosity value ligaments between cavities fail in shear. The rate of this part of the failure process depends on how much the remote tension is above P_c. We assume here that in a dynamic situation this rate is high, and that just crossing P_c may signify failure in tension. There is a branch of failure modeling that follows void growth beyond P_c to the final failure event, see chapter 7 in [6]. As this part is rather complex, we avoid it here by lumping it into a rate dependent damage term, as described later.

For non symmetric remote tension there is no analytical solution to the cavitation problem, and we resort to computer simulations, using the Lagrange processor of the old commercial hydro code 2D-PISCES in axial symmetry. The computation sample is a cylinder 20 mm long and of 20 mm diameter. At the origin there is a cylindrical pore 2 mm long and of 2 mm diameter. The initial porosity is therefore 1/1000, which seems low enough. The material is aluminum with a low value of constant flow stress Y=0.2 GPa. On the outer boundary we put a tensile boundary stress, σ_x on the axial boundary and σ_r on the radial boundary. We use low values of Y to avoid high stresses near the boundaries. Although we use a hydro code, the solution can be considered quasi static, as velocities are rather low. We monitor the velocity at the corner of the initial cavity. Generally, when boundary stresses are low, the corner velocity first increases and then decreases to zero; but when they are high, the corner velocity tends to accelerate. The border between deceleration and acceleration signifies the cavitation threshold.

It turns out that when the remote boundary stress components are about equal, cavitation threshold (relative to Y) is highest. We show the results of all runs in figure 1.

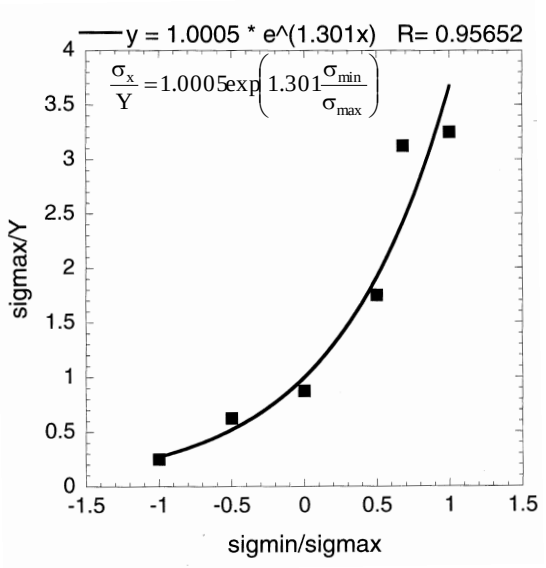

Figure 1. Summary of cavitation threshold results from the simulations.

We see that the remote stress components at the onset of cavitation can be approximated by a single curve when plotted by (σ_{max}/Y) as function of ($\sigma_{min}/\sigma_{max}$). We see from figure 1 that: (1) The highest

tensile stress at the onset of cavitation is for isotropic tension, and the cavitation threshold decreases as the remote stress state is less isotropic, (2) Cavitation may occur as long as the maximal principal stress component is positive (tensile), even if the other principal stress components are negative (compressive), (3) Cavitation and failure in tension depend on shear strength, and this provides a link between failure in tension and failure in shear.

Our simulations are 2D and include only two remote principal stress components. It is safe to assume that cavitation threshold would depend on all three principal stress components. Evaluation of this dependence calls for 3D simulations.

3. Tension-shear failure model

From the simulations above we deduce (figure 1) that cavitation threshold can be expressed by:

$$\frac{\sigma_{max}}{Y} = A\exp\left(\alpha\frac{\sigma_{min}}{\sigma_{max}}\right) \tag{1}$$

where A and α are curve fitting parameters given in figure 1. The flow stress Y can of course depend on pressure, temperature, effective plastic strain, and strain rate, as usual. To demonstrate how the model works, we use a single computational cell tool. The cell is a box with dimensions a_x, a_y, a_z, all initially equal to 1 mm, and we specify the velocities of the box faces that do not go through the origin u_x, u_y, u_z. We use u_x=10 m/s, and give different values to the other velocity components. To compute the rate of change of the average stress deviator components we first compute:

$$\begin{aligned} &d_i \cong u_i/a_i \;;\; i = x,y,z \;;\; \delta_i = d_i - \tfrac{1}{3}\sum d_i \\ &\sigma_{eq}^2 = \tfrac{3}{2}\sum s_i^2 \;;\; d_{eff}^p = A_p\left(\sigma_{eq} - Y\right);\; \sigma_{eq} > Y \\ &\lambda = \tfrac{3}{2}d_{eff}^p/\sigma_{eq} \;;\; d_i^p = \lambda s_i \;;\; \delta_i^e = \delta_i - d_i^p \\ &\dot{W}_p = V\sum s_i d_i^p \end{aligned} \tag{2}$$

where d_i=deformation rate, δ_i=deformation rate deviator, s_i=stress deviator, σ_{eq}=equivalent stress, d^p_{eff}=effective plastic deformation rate, Y=quasi static flow stress, W_p=dissipative plastic work per unit mass, and A_p=overstress viscoplastic parameter. Using these relations we get a system of 9 ODEs:

$$\begin{aligned} &\dot{a}_i = u_i \;;\; \dot{s}_i = 2G\delta_i^e \\ &\dot{V} = V\sum d_i \;;\; \dot{\varepsilon}_{eff}^p = d_{eff}^p \\ &\left(\partial E/\partial P\right)\dot{P} = \left(P + \partial E/\partial V\right)\dot{V} + \dot{W}_p \end{aligned} \tag{3}$$

where G=shear modulus, and where the partial derivatives are derived from a Gruneisen EOS referenced to the shock Hugoniot. We integrate the ODE system with a standard ODE solver. In the examples the cavitation (or failure) threshold (σ_f) is given by σ_{max} of equation (1), and the material is aluminum. Figure 2a is for isotropic tension, u_x=u_y=u_z=10 m/s, and figure 2b is for uniaxial strain tension u_y=u_z=0, u_x=10 m/s. In both figures we show $\sigma_{max}(t)$ relative to σ_f.

We see from figure 2a that the tensile stress crosses the failure stress after about 0.5 μs. Had the tensile process been slow, this would indicate failure in tension upon crossing. But as this is a dynamic process (although not very fast), the state point may go beyond the failure stress (overstress). But after it crosses, damage accumulates at a rate that increases with overstress. We haven't switched on damage accumulation in this run (see the effect of damage accumulation in figure 4).

From figure 2b we see that qualitatively, the result is not much different from that of figure 2a. In another run (not shown here) we used u_y=u_z=-3 m/s, but the overall picture still stayed the same.

In all these runs the effective plastic strain upon crossing the cavitation threshold is quite low, which is in disagreement with tests used in the literature to calibrate failure models. Recalling that all these tests are in uniaxial or plane stress, we transform our single cell equations accordingly, to represent uniaxial or plane stress. We use stress free ghost cells outside our computational cell, and compute the face velocities by:

$$\dot{u}_y = \sigma_y/(\rho a_y);\ \dot{u}_z = \sigma_z/(\rho a_z) \tag{4}$$

This adds two more ODEs to our system.

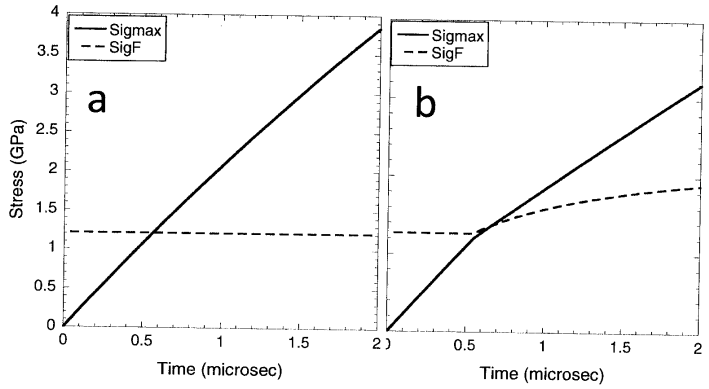

Figure 2. Histories of the tensile stress and the failure stress. Figure 2a is for isotropic tension with $u_x=u_y=u_z=10$ m/s. Figure 2b is for uniaxial strain tension with $u_y=u_z=0$, $u_x=10$ m/s.

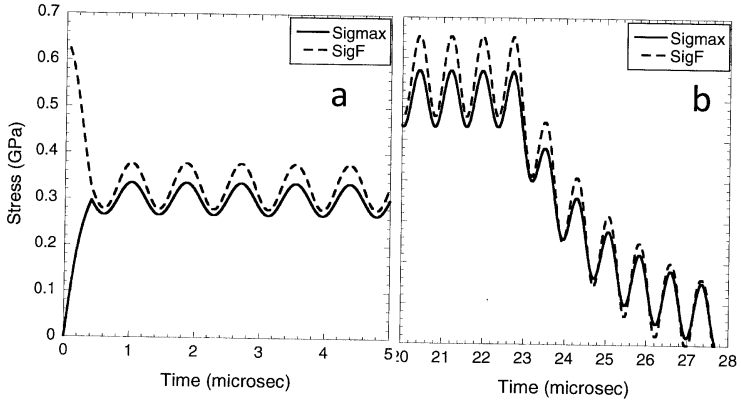

Figure 3. Histories of the maximal tensile stress and the failure stress for uniaxial tension with simultaneous failure in shear. Figure 3a shows the first 5 μs. Figure 3b shows the last 8 μs. The oscillations are an artifact of the way we enforce the uniaxial stress state using equation (4).

In figure 3 we show the result of such a uniaxial stress run. We added to this run failure in shear by letting the flow stress decrease linearly to zero between effective plastic strain values of 0.30 and 0.32. We see from figure 3 that in a uniaxial stress state the tensile stress does not cross the failure stress. Upon failure in shear the tensile failure stress drops, and so does the stress. The oscillations in figure 3 are an artifact of the way we enforce the uniaxial stress state using equation (4).

Upon crossing the cavitation threshold we accumulate damage by:

$$\begin{aligned} &\dot{D} = A(\sigma_{max} - \sigma_f);\ \dot{F} = B\,D^{\beta} \\ &\Delta\sigma_i = -\sigma_i \dot{F};\ \dot{Y} = -Y\,\dot{F} \end{aligned} \tag{5}$$

where D=damage, and A, B, β are material parameters. σ_i=any of the stress components, and $\Delta\dot{\sigma}_i$ =additional rates of change of stress components caused by damage. In figure 4 we show results of a run as in figure 2a, but including damage accumulation. We use A=1. $(GPa*\mu s)^{-1}$, B=100./μs, β=2.

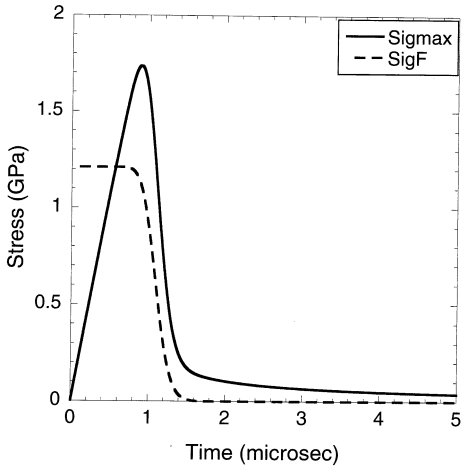

Figure 4. Histories of the tensile stress and the failure stress for isotropic tension as in figure 2a, but including damage accumulation.

4. Summary

Ductile materials can fail in shear and/or in tension, and these two modes of failure are caused by different mechanisms. Failure in shear occurs through shear localization and formation of shear bands, and results in loss of shear strength. Failure in tension occurs by spontaneous void growth, and results in loss of tensile strength and of shear strength.

We propose here a combined tension-shear failure model for ductile materials. We identify failure in tension as the onset of cavitation (spontaneous void growth) by a remote tension field, and determine the cavitation threshold using hydro code simulations with various remote field stress states. It turns out that cavitation threshold depends on the flow stress (shear strength), and in this way failure in tension becomes coupled to failure in shear.

We apply our model in a single cell computational tool. This is a 3D box for which we specify the velocities of the faces, and/or the stresses outside these faces, and compute average box values of state and kinematic variables. We show several examples of how the model works, and how failure in tension and shear may interact.

5. References

[1] Bai Y and Wierzbicki T 2008 A New Model of Metal Plasticity and Fracture with Pressure and Lode Dependence *Int. J. Plasticity* **24** 1071-1096.
[2] Wierzbicki T, Bao Y, Lee W and Bai Y 2005 Calibration and Evaluation of Seven Fracture Models *Int.J.Mech. Sci.* **47** 719-743
[3] Bao Y and Wierzbicki T. 2004 On Fracture Locus in the Equivalent Strain and Stress Triaxiality Space *J. Mech. Sci.* **46** 81-98
[4] Johnson J R and Cook W H 1985 Fracture Characteristics of Three Metals Subjected to Various Strains, Strain Rates, Temperatures and Pressures *Eng. Fract. Mech.* **21** 31-48
[5] Bishop R F, Hill R and Mott N F 1945 The Theory of Indentation and Hardness Tests *Proc. Phys. Soc.* **57** pp.149
[6] Antoun T 2003 Spall Fracture Springer-Verlag New York, Inc.